Supporting Information for "The seismic signature of upper-mantle plumes: application to the northern East African Rift"

Chiara Civiero[1], John J. Armitage[2], Saskia Goes[3], James O. S. Hammond[4]

[1]Dublin Institute for Advanced Studies (DIAS), Dublin D02 Y006, Ireland

[2]Institut de Physique du Globe, Université de Paris, F-75005 Paris, France

[3]Department of Earth Science and Engineering, Imperial College London, London, UK

[4]Department of Earth and Planetary Sciences, Birkbeck, University of London, London, UK

Contents of this file

Introduction

The Supporting Information comprises:

- Table S1 lists all the model parameters.

- Fig. S1 shows the seismic stations and the earthquakes used in the P- and S-wave tomography.

- Fig. S2 illustrates the wavelength for Rayleigh Bénard convection according to the Rayleigh number.

- Fig. S3 compares the patterns of Rayleigh Taylor destabilisation of a 100 °C hot layer for two different aspect ratios (3x3x1 and 4x4x1).

- Fig. S4 shows the volumes used for the tomographic inversion, for one of the numerical models and for the region of interpretation.

- Figs. S5 and S6 are the same tests shown in Figs. 4 (N7 with a 100 °C thermal boundary layer) and 5 (N9 with a 400 °C thermal boundary layer) below the MER.

- Fig. S7 illustrates the 3D plot of the plume model N10.

Parameter	Value	Description
B	0.5	Bouyancy number for the lithosphere
g	$9.8\,\mathrm{m\,s^{-2}}$	Acceleration due to gravity
H	700 km	Model depth
p		Pressure
Ra		Initial Rayleigh number
T		Temperature
ΔT	1350 °C	Asthenosphere temperature
ΔT_e		Temperature anomaly
α	$3.3 \times 10^{-5}\,\mathrm{K^{-1}}$	Coefficient of thermal expansion
κ	$10^{-6}\,\mathrm{m^2\,s^{-1}}$	Thermal diffusivity
ρ_m	$3340\,\mathrm{kg\,m^3}$	Mantle density
η_0		Scaling viscosity
	Newtonian Rheology	
E	$120\,\mathrm{kJ\,mol^{-1}}$	Activation energy
A_{ref}	$2.2 \times 10 - 5$	Normalizing factor
	Non-Newtonian Rheology	
E	$523\,\mathrm{kJ\,mol^{-1}}$	Activation energy
V	$4\,\mathrm{cm^3\,mol^{-1}}$	Activation volume
n	3.6	Stress exponent
A_{ref}	1.47×10^{-16}	Normalizing factor

Table S1. Model parameters.

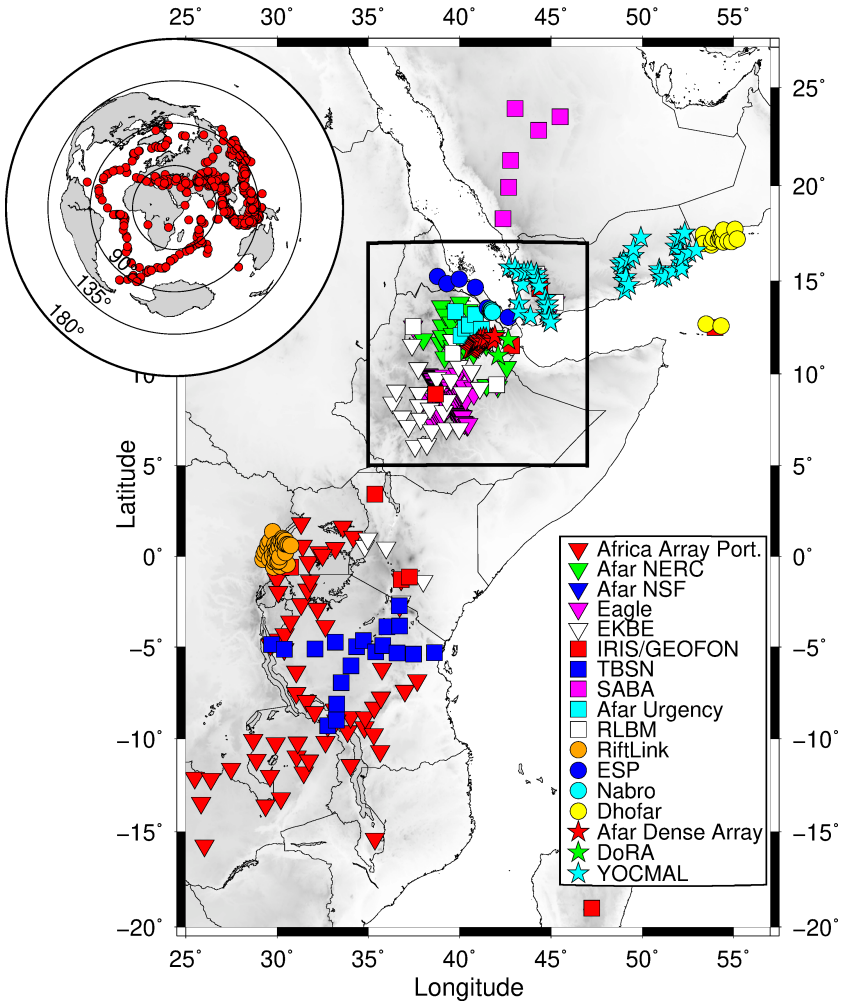

Figure S1. Distribution of sources (red dots in inset) and stations (main map) used in the P-wave tomographic study. The stations are colour coded according to their network and cover the region from Madagascar in the south to Saudi Arabia in the north. The black rectangle shows the area on which we concentrate our analyses and interpretation. Source-receiver distances shown by the circles on the inset are from the centre of the black rectangle.

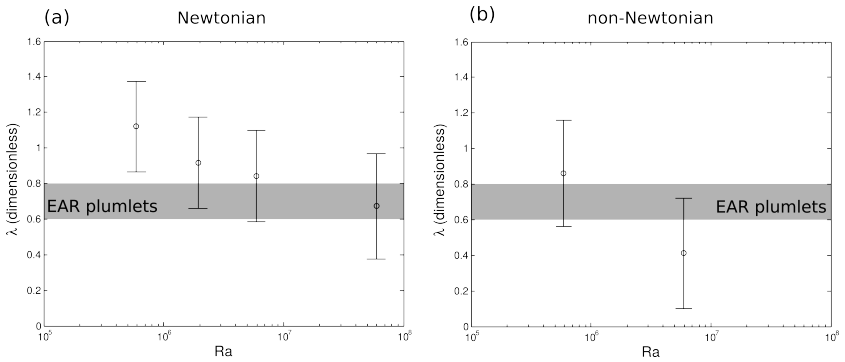

Figure S2. Dimensionless wavelength for Rayleigh Bénard convection as a function of Raleigh number. (a) Newtonian models, showing the classic power law dependence between wavelength and Ra. The grey shaded area shows the estimate for the wavelength of the slow Vs anomalies below EAR, made dimensionless by dividing by the depth to the 660 km depth seismic discontinuity. If these instabilities are due to Raleigh Bénard convection, we would require a low viscosity (high *Ra*). (b) Non-Newtonain models, showing a stronger dependence on *Ra*. However in this case at $Ra > 10^7$, the plumes become difficult to detect given the plume tails are very thin. If the upper mantle is dominantly non-Newtonian, EAR plumlets are consistent with a higher viscosity (lower *Ra*).

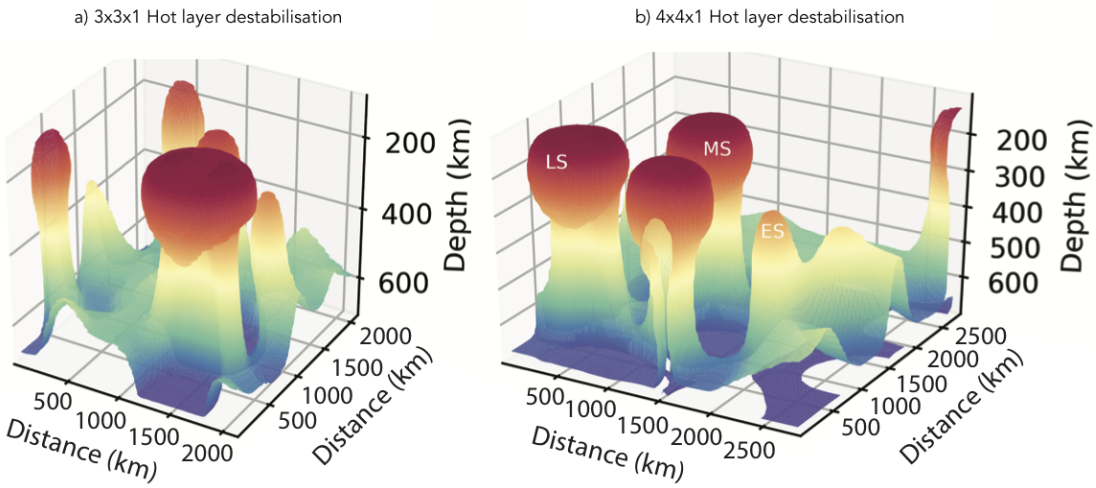

Figure S3. Comparison of patterns of destabilisation of a 100 °C hot layer for a 3x3x1 and 4x4x1 Cartesian box. Labeled are ES - early-stage plumelet; MS - mid-stage plumelet; and LS - late-stage plumelet. Note that the aspect ratio is distorted.

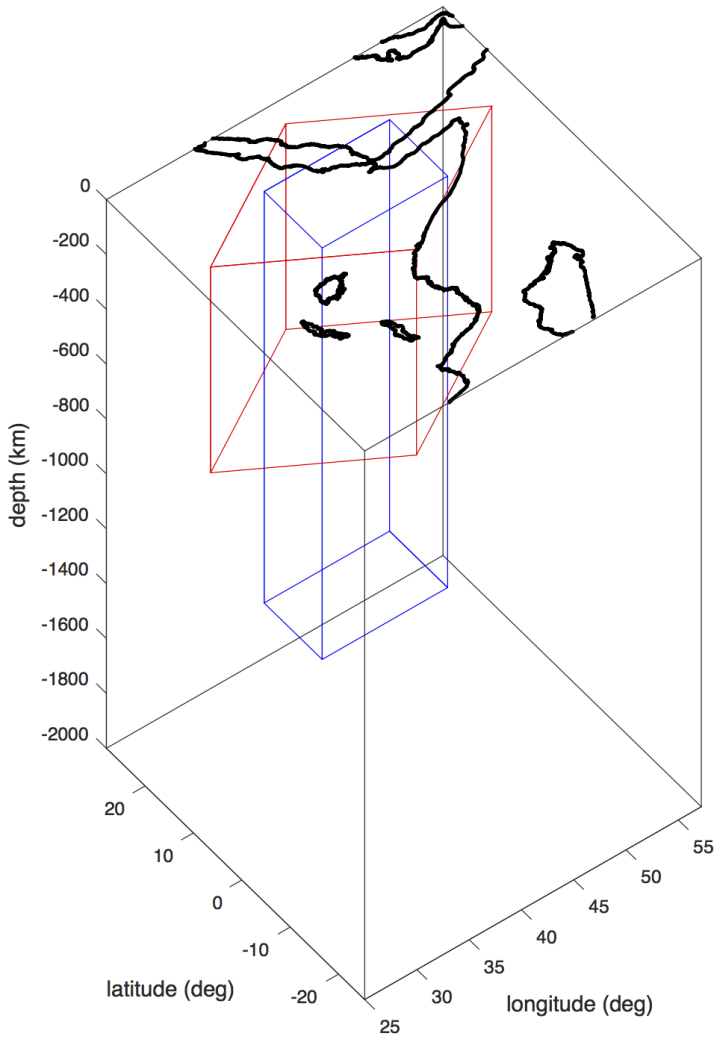

Figure S4. 3D perspective figure illustrating the relative sizes and locations of the tomographic and numerical model boxes. The black volume is the whole volume for the tomographic inversion. The red box is the approximate volume of the numerical models used to perform the plume resolution tests. This orientation in space places the synthetic low-velocity structures at the same position as the imaged tomographic low-velocity anomalies beneath Afar and MER. The blue volume represents our region of interpretation, parameterised with a finer grid than outside.

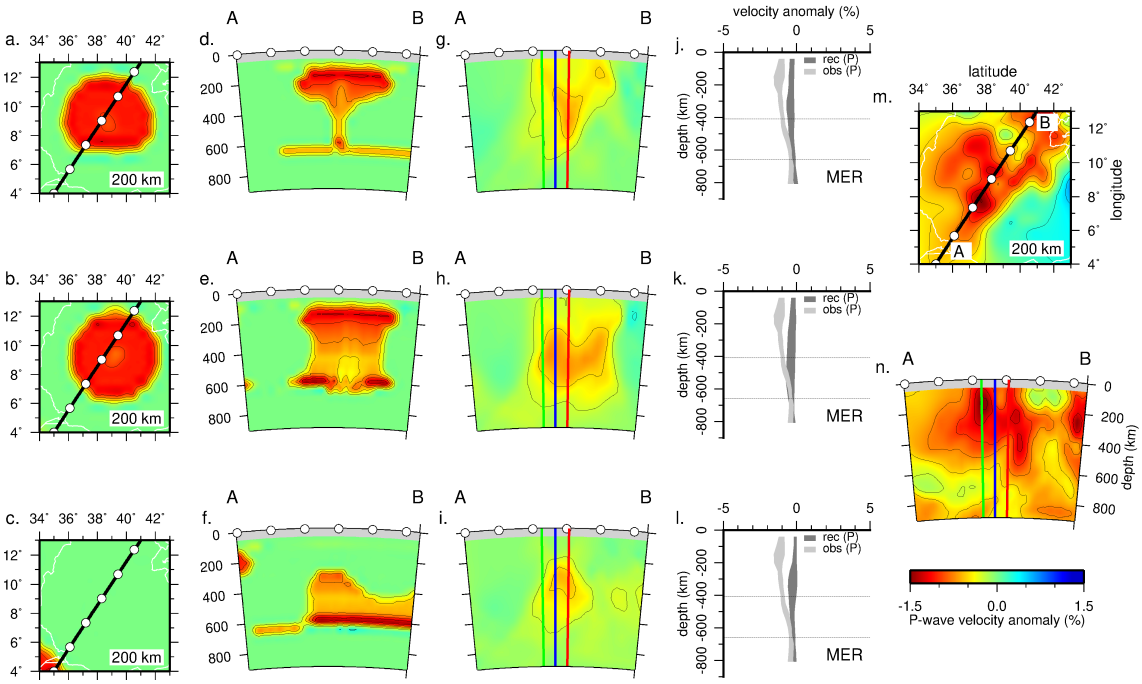

Figure S5. Same as Fig. 4 below the MER. Contours are drawn every 0.25%. White points indicate the distance every 2°.

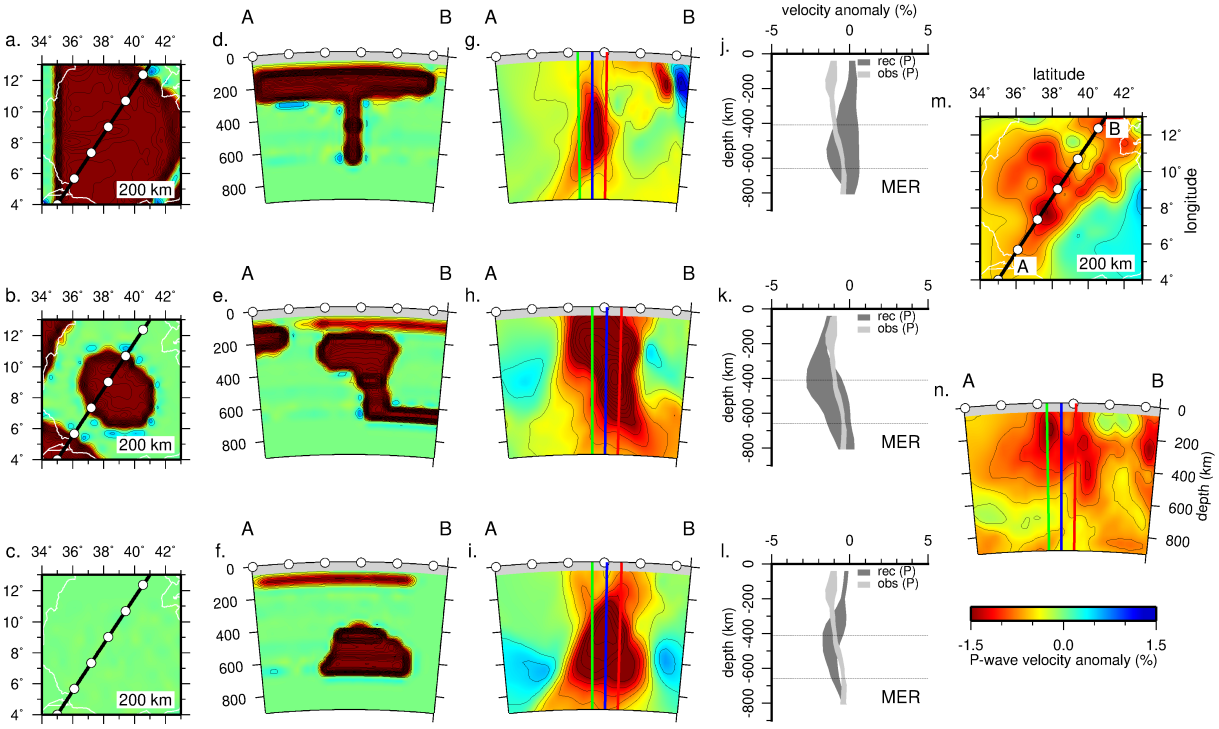

Figure S6. Same as Fig. 5 below the MER. Contours are drawn every 0.25%. White points indicate the distance every 2°.

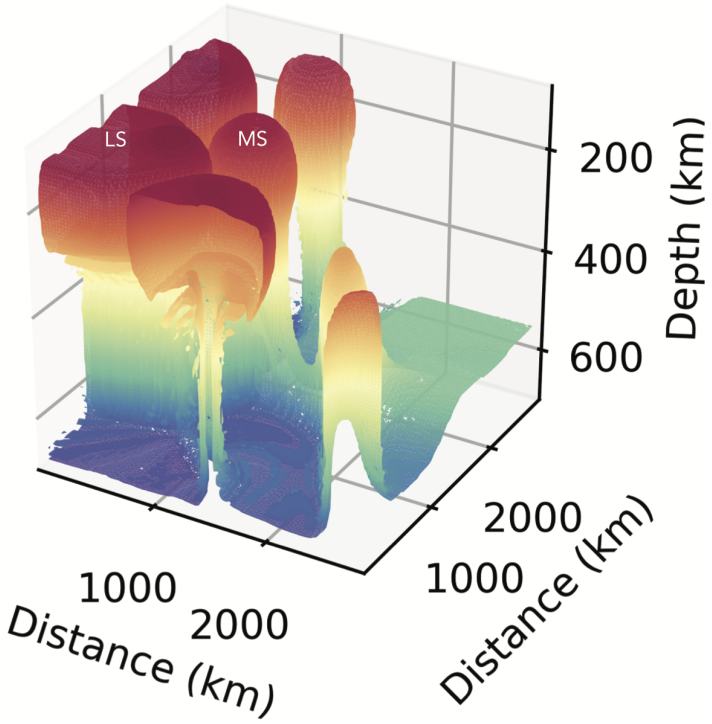

Figure S7. Snap-shot of the three-dimensional plume model N10 (2800x2800x700 km). Plumes with different morphologies and stages of evolution form and rise from the initial hot boundary layer at the base of the box. The two structures labelled as MS, and LS (middle and late-stage plumes) in the box are used as input for our resolution tests.